Crossover from Coherent to Incoherent Electronic Excitations in the Normal State of $Bi_2Sr_2CaCu_2O_{8+\delta}$

A. Kaminski,[1,2,3] S. Rosenkranz,[1,2] H. M. Fretwell,[3] Z. Z. Li,[4] H. Raffy,[4] M. Randeria,[5] M. R. Norman,[2] and J. C. Campuzano[1,2]

[1]*Department of Physics, University of Illinois at Chicago, Chicago, Illinois 60607, USA*
[2]*Materials Science Division, Argonne National Laboratory, Argonne, Illinois 60439, USA*
[3]*Department of Physics, University of Wales Swansea, Swansea, SA2 8PP, United Kingdom*
[4]*Laboratoire de Physique des Solides, Université Paris-Sud, 91405 Orsay, France*
[5]*Tata Institute for Fundamental Research, Homi Bhabha Road, Mumbai 400005, India*

(Received 23 October 2002; published 21 May 2003)

Angle resolved photoemission spectroscopy (ARPES) and resistivity measurements are used to explore the overdoped region of the high temperature superconductor $Bi_2Sr_2CaCu_2O_{8+\delta}$. We find evidence for a new crossover line in the phase diagram between a coherent metal phase, for lower temperatures and higher doping, and an incoherent metal phase, for higher temperatures and lower doping. The former is characterized by two well-defined spectral peaks in ARPES due to coherent bilayer splitting and superlinear behavior in the resistivity, whereas the latter is characterized by a single broad spectral feature in ARPES and a linear temperature dependence of the resistivity.

DOI: 10.1103/PhysRevLett.90.207003 PACS numbers: 74.25.Dw, 74.25.Fy, 74.72.Hs, 79.60.Bm

The normal state of optimal and underdoped high temperature superconductors (HTSCs) exhibits anomalous transport and spectroscopic properties which have long been recognized as one of the central mysteries of the field [1,2]. The electronic excitations are unlike those of conventional metals, where one can think of dressed electrons as quasiparticles. Instead, the response in the normal state of the HTSCs is incoherent, with no identifiable single-particlelike excitations. The key question is how the strange metal evolves into the conventional one at high doping. Some models propose that the incoherent normal metal represents a new state of matter, with a crossover to more conventional behavior [3]. Others suggest that the incoherent state is a result of underlying competing interactions, and therefore its behavior evolves continuously from the conventional one [4].

Here we provide the first spectroscopic evidence for a new crossover line in the phase diagram of the HTSCs between the low temperature, overdoped side with coherent electronic excitations, and the high temperature, underdoped side, where this coherence is lost. We conclude that the electronic excitations in these two regions of the phase diagram are qualitatively different.

For our purposes, we use angle resolved photoemission (ARPES) and resistivity measurements of $Bi_2Sr_2CaCu_2O_{8+\delta}$ (Bi2212), which possesses two CuO_2 layers (a bilayer), and thus the issue of coherence can be probed by not only examining its planar properties as a function of doping and temperature, but also by looking for the presence of bilayer splitting; if the motion of electrons within the bilayer is coherent, then we expect the formation of antibonding (A) and bonding (B) states. These are the antisymmetric and symmetric combinations of the layer wave functions with energies $\epsilon_{A(B)}(\mathbf{k}) = \epsilon(\mathbf{k}) \pm t_\perp(\mathbf{k})$, where $\epsilon(\mathbf{k})$ is the planar dispersion and $t_\perp(\mathbf{k})$ the interplanar coupling. As the CuO_2 planes in Bi2212 are separated by only 3.17 Å, electronic structure calculations predict a sizable bilayer splitting of order 0.3 eV [5]. In the coherent regime, the primary effect of interactions would be to renormalize the splitting to a smaller value, without qualitatively affecting the spectrum. On the other hand, if the interactions are sufficiently strong, then we expect the coherent behavior within each plane, as well as the coherent motion within the bilayer, to be destroyed [1]. The in-plane effect would be reflected in both the ARPES spectral line shape and in the temperature dependence of the planar transport. The out-of-plane effect would be a loss of the coherent bilayer splitting.

Epitaxially grown thin films of Bi2212 [6] were characterized by resistivity and x-ray diffraction and then transferred into the ARPES chamber without baking so as not to alter the doping. These films have the very useful feature of displaying small signals from the structural superlattice distortion ($< 3\%$), which otherwise would complicate the interpretation of ARPES data in the vicinity of the $(\pi, 0)$ point of the Brillouin zone [7]. This is particularly important for us, since bilayer splitting is maximal at $(\pi, 0)$ [8–11], as shown in Fig. 1(a).

ARPES measurements were carried out at the Synchrotron Radiation Center in Wisconsin with an energy resolution of 30 meV and a momentum resolution of 0.01 $Å^{-1}$. The ARPES intensity as a function of the planar momentum $\mathbf{k}$ and energy ω (measured with respect to the chemical potential) is given by [12] $I(\mathbf{k}, \omega) = I_0(\mathbf{k}) f(\omega) A(\mathbf{k}, \omega)$ (convolved with the resolution function). Here I_0 is an intensity prefactor, f is the Fermi function, and A is the single particle spectral function, which measures the probability of removing or adding an electron from the system. The peak in $A(\mathbf{k}, \omega)$ measures

the energy of the electronic excitation, while its linewidth is inversely proportional to the lifetime. Since the ARPES line shape is "chopped off" by $f(\omega)$, we sometimes divide our data by a resolution broadened Fermi function (the leading edge of polycrystalline Au in contact with the sample). This allows us to focus directly on $A(\mathbf{k}, \omega)$.

Figure 1(b) shows raw ARPES data for an overdoped sample ($T_C = 52$ K) at $T = 100$ K, along a momentum cut centered at the $(\pi, 0)$ point of the Brillouin zone. In addition, Fig. 1(c) shows the same data divided by $f(\omega)$.

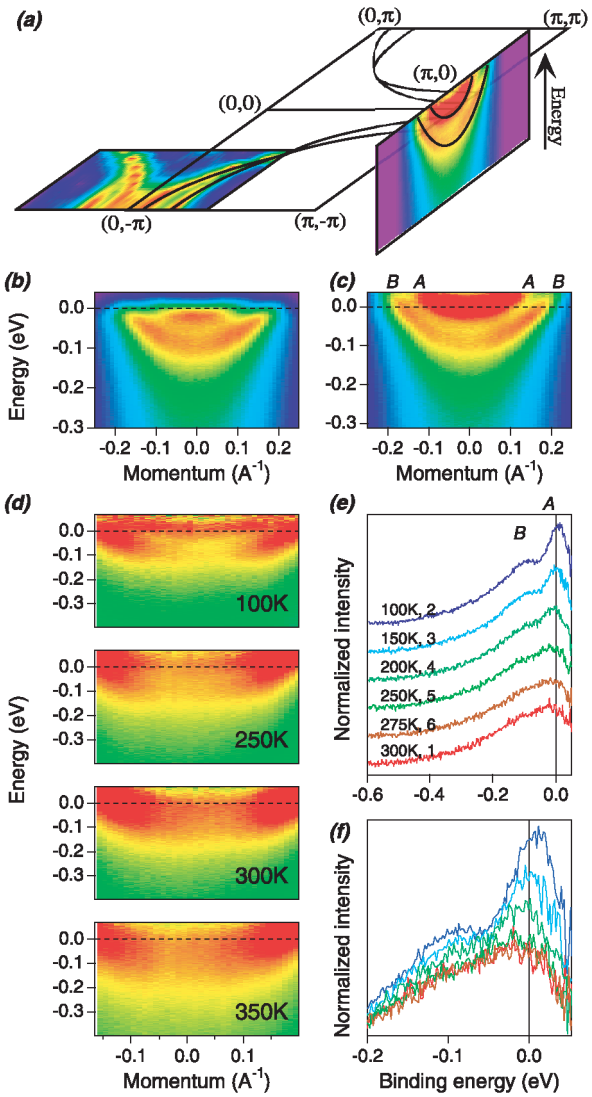

FIG. 1 (color online). ARPES data for overdoped ($T_C = 52$ K) Bi2212 samples S1 and S2. (a) Intensity versus momentum and energy for $T = 100$ K. The two solid curves represent the bilayer split Fermi surface sheets and "bands." (b) Intensity for momenta along $(\pi, 0) - (\pi, \pi)$ for S1 at $T = 100$ K, with plots centered at $(\pi, 0)$. (c) The same data divided by the Fermi function. (d) Same as in (c) for S2, at various temperatures. (e) Spectra for S2 at $(\pi, 0)$ (divided by the Fermi function) at various temperatures. (f) All curves of (e) overlapped to demonstrate that the coherent features disappear by loss of intensity without broadening as the temperature increases.

The data in Fig. 1(c) reveal two dispersing bands due to the bilayer splitting, with the A band close to, and the B band well below, the chemical potential at $(\pi, 0)$. In Fig. 1(d), we show data such as that in Fig. 1(c) (divided by the Fermi function) for another sample with the same T_C as a function of temperature. The bilayer splitting can clearly be seen at 100 K; however, above 250 K the two bands are no longer observed. To obtain more precise information, in Fig. 1(e) we show the temperature dependence of the spectral function at $(\pi, 0)$ as a function of energy (raw data divided by the Fermi function). The sample was temperature-cycled when taking the data to ensure that the observed effect is intrinsic and not due to the sample aging (the numbers in the legend indicate the order of measurement). At 100 K, one sees clearly the presence of two peaks, a sharp A peak near the chemical potential and a broader B peak at about 100 meV below. These two peaks ride on top of an underlying broad incoherent feature. As seen from Fig. 1(f), both peaks lose intensity with temperature *without broadening,* until only the underlying broad *temperature independent* feature remains at 250 K. This behavior cannot be explained simply by thermal broadening.

We thus argue that above 250 K the system no longer exhibits coherent excitations, both in regards to inverse lifetime (spectral peak widths) and bilayer splitting

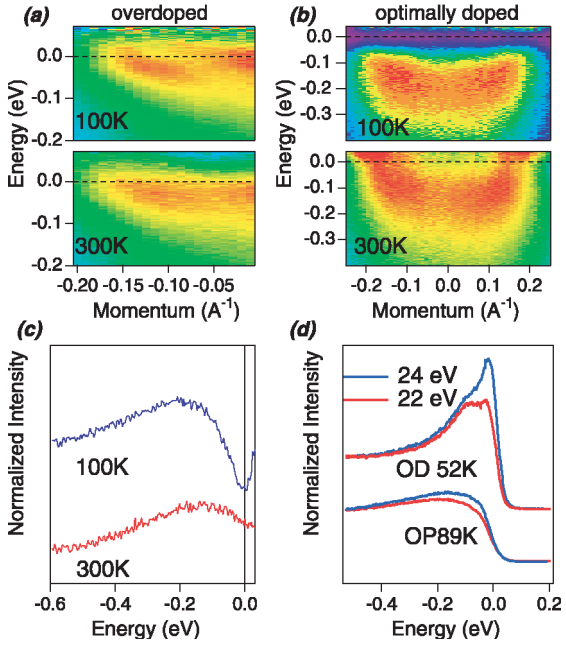

FIG. 2 (color online). ARPES data for samples at various dopings. (a) As in Fig. 1(d), but for an overdoped ($T_C = 75$ K) sample. (b) As in Fig. 1(d), but for an optimal doped ($T_C = 89$ K) sample (at 100 K the intensity at the chemical potential is suppressed due to the pseudogap). (c) Spectrum at $(\pi, 0)$ (divided by the Fermi function) for an optimal doped ($T_C = 89$ K) sample. (d) Raw data at $(\pi, 0)$ at two different photon energies for an overdoped ($T_C = 52$ K) sample and an optimal doped ($T_C = 89$ K) sample at $T = 100$ K.

(appearance of two separate spectral peaks). That is, the data indicate that *both* in-plane and out-of-plane coherence are lost together [13]. Moreover, these effects show a strong doping dependence, as we demonstrate next.

In Fig. 2(a), we show data such as that in Fig. 1(d), but for an overdoped ($T_C = 75$ K) sample. Again, note the presence of bilayer splitting at 100 K which is not visible at 300 K. We can contrast this behavior with that of an optimally doped sample ($T_C = 89$ K) shown in Fig. 2(b), where the intensity plots do not indicate the presence of bilayer splitting, even at 100 K. This is further illustrated in Fig. 2(c), where again the spectrum at $(\pi, 0)$ (divided by the Fermi function) is shown. At 100 K, only a single broad peak is seen, with no presence of bilayer splitting, indicating incoherent behavior. Instead, a pseudogap is seen, centered at the chemical potential, which fills in as the temperature is increased. An important check can be made by analyzing the photon energy dependence of the data. It has been recently observed that the spectral line shape changes as a function of photon energy for overdoped samples due to the relative weighting of the *A* and *B* peaks [10,11]. This is clearly seen in Fig. 2(d), where data at $(\pi, 0)$ for the overdoped sample of Fig. 1 are shown for two different photon energies. In contrast, for the optimal doped sample, we observe only a very small change over a wide range of photon energies (15–50 eV). This indicates the absence of bilayer splitting.

It is also useful to plot the data as a function of momentum for fixed energy (momentum distribution curve, or MDC). In Fig. 3 we show such plots for a few values of the binding energy, at low and high temperatures, for two samples, an overdoped sample such as that in Fig. 1 and another optimal doped sample ($T_C = 89$ K). At 100 K and energies close to the chemical potential, the overdoped MDC has four peaks [Fig. 3(a)]. The two peaks closest to the center of the plot correspond to the *A* band, while the two peaks on the outside correspond to the *B* band. As the binding energy increases, the two *A* peaks approach each other and then merge into a single peak, which then disappears at still higher energies. This is the expected behavior of MDCs close to the bottom of a band and is also observed for the *B* peak at even higher binding energies. However, at high temperatures only two peaks are observed, regardless of binding energy [Fig. 3(a)]. This can be contrasted with the optimally doped sample, where only two peaks are visible in the MDCs, whether at 100 or 300 K [Fig. 3(b)]. In addition, the MDC profiles of Fig. 3(b) are also independent of energy, unlike those in Fig. 3(a).

We now connect our ARPES observations with in-plane transport data taken on the same films using the standard four-probe method. In Fig. 4 we plot the resistivity as a function of temperature for the optimally doped [Fig. 4(a)] and overdoped [Fig. 4(b)] samples of Fig. 3, with the blue line a linear fit to the high temperature data. At high temperatures, both samples exhibit a linear T resistivity which has been linked to the absence

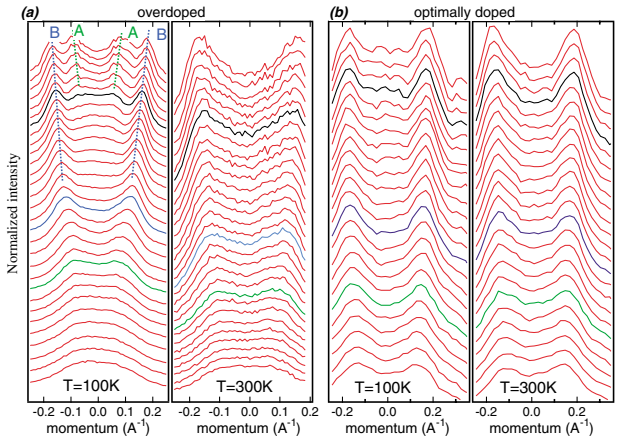

FIG. 3 (color online). Momentum distribution curves (MDCs) along $(\pi, 0) - (\pi, \pi)$ for various energies. The black curves are at the chemical potential, the blue at -50 meV, and the green at -100 meV. The curves for the energies above -50 meV are spaced every 5 meV and remaining curves every 10 meV. (a) Overdoped ($T_C = 52$ K) sample at 100 K (*A* and green dotted lines mark antibonding peaks; *B* and blue dotted lines mark bonding peaks) and 300 K. (b) Optimal ($T_C = 89$ K) sample at 100 and 300 K. The data are quite noisy at 100 K close to the chemical potential because of the intensity being suppressed due to the pseudogap.

of coherent quasiparticles [1,2]. For the optimally doped sample, this behavior continues to near T_C, with the rounding just above T_C due to fluctuation effects. In contrast, the overdoped sample shows strong deviations from linearity, which set in at about 250 K. These results can be understood more easily by plotting the derivative of the resistivity, which emphasizes the strength of the inelastic scattering contribution. One can see that while

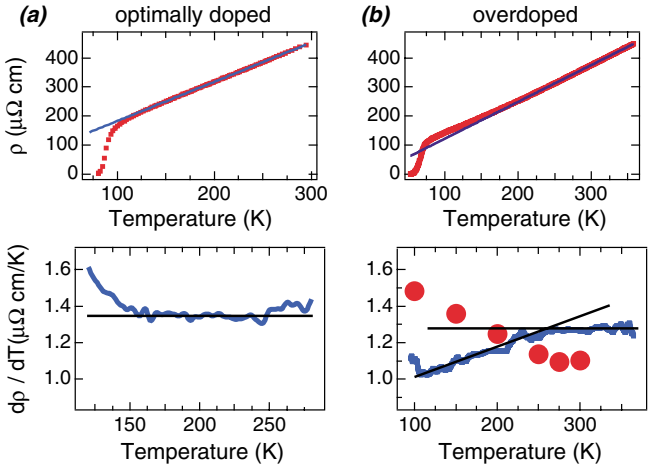

FIG. 4 (color online). Resistivity data. The blue lines denote linear fits to the high temperature data for (a) optimal doped ($T_C = 89$ K) and (b) overdoped ($T_C = 52$ K) samples (top graphs). The bottom plots are the temperature derivative of the resistivity for the two dopings, with black lines guides to the eye. Red dots on the bottom right plot are the ARPES intensities from Fig. 1(e).

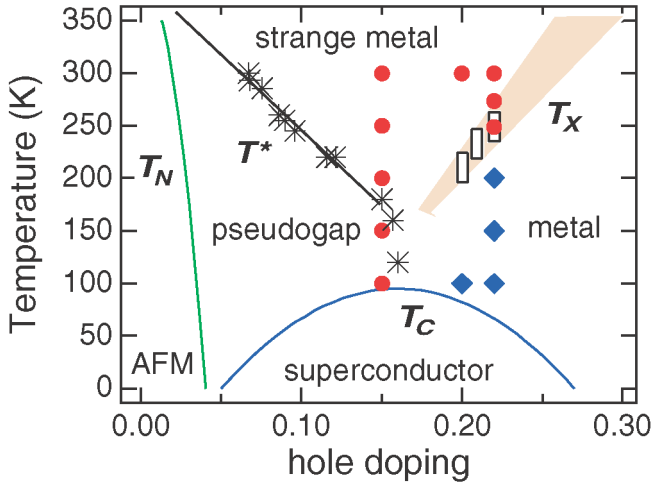

FIG. 5 (color online). Phase diagram for the HTSCs. The strange metal/pseudogap transition (black stars) and strange metal/metal crossover (black squares) are obtained from the departure from linear T resistivity. The red dots correspond to ARPES data where bilayer splitting was not observed; the blue diamonds correspond to ARPES data showing bilayer splitting.

the optimally doped sample shows a constant derivative, the overdoped sample shows a change in the derivative at 250 K. Below this temperature, the derivative decreases monotonically. This superlinear behavior of the resistivity below 250 K indicates the presence of coherent excitations. We note the strong correlation of these observations with ARPES. In the optimally doped sample, sharp spectral peaks begin to appear only at temperatures slightly above T_C. And in the overdoped sample [Fig. 1(e)], the sharp A peak disappears above 250 K. As we show in the bottom right panel in Fig. 4, the ARPES intensity is inversely related to $d\rho/dT$. In particular, the intensity becomes constant when the resistivity becomes linear.

Based on our results, we show in Fig. 5 a proposed phase diagram for the HTSCs. The crossover between the pseudogap phase and the strange metal phase has been studied in the past, both by ARPES [14] and transport [6]. What we have shown here is the presence of a new crossover line, between a conventional metal phase on the overdoped side of the phase diagram and the strange metal phase, seen from both spectroscopic and transport measurements. The two crossover lines (pseudogap/strange metal and metal/strange metal) were determined by the departure from linear T resistivity. In all cases, the crossover lines were verified by ARPES, with the pseudogap line being determined by the closing of the leading edge gap at $(\pi, 0)$ and the metal line by the loss of the sharp (A) peak at $(\pi, 0)$.

The crossover line we have found from the loss of coherence has been long predicted on theoretical grounds. Slave boson studies of the t-J model [3,15] predict a phase diagram very similar to Fig. 5, with the crossover line between the strange metal and metal phases marking the "condensation of holons" (i.e., for temperatures below this, the doped holes have phase coherence). However, a similar crossover to the one observed here may also be expected near a quantum critical point [16], with the "ordered" region corresponding to the pseudogap, the disordered region to the conventional metal, and the quantum critical regime to the strange metal phase. Further studies are needed to distinguish these possibilities.

In conclusion, our data show the presence of a coherent normal metal in overdoped samples and that this state crosses over into an incoherent metal at higher temperatures. We emphasize that the ARPES data indicate a loss of *both* in-plane and out-of-plane coherence. Furthermore, this crossover temperature increases with doping. Our studies indicate that the normal state of the HTSCs, with its various phases, is a much richer field of study than even its exotic superconducting state and has strong implications for the many body theory of electrons in reduced spatial dimensions.

This work was supported by the NSF DMR 9974401 and the U.S. DOE, Office of Science, under Contract No. W-31-109-ENG-38. The Synchrotron Radiation Center is supported by NSF DMR 9212658. A. K. is supported by the Royal Society U.K., S. R. in part by the Swiss National Science Foundation, and M. R. by the Indian DST through the Swarnajayanti scheme. We acknowledge helpful discussions with P. D. Johnson and A. J. Leggett.

[1] P. W. Anderson, *The Theory of Superconductivity in the High-T_c Cuprates* (Princeton University Press, Princeton, 1997).
[2] C. M. Varma *et al.*, Phys. Rev. Lett. **63**, 1996 (1989).
[3] P. W. Anderson, Science **235**, 1196 (1987); G. Kotliar and J. Liu, Phys. Rev. B **38**, 5142 (1988); H. Fukuyama, Prog. Theor. Phys. Suppl. **108**, 287 (1992).
[4] R. B. Laughlin, Adv. Phys. **47**, 943 (1998).
[5] S. Massidda, J. J. Yu, and A. J. Freeman, Physica (Amsterdam) **152C**, 251 (1988).
[6] Z. Konstantinovic, Z. Z. Li, and H. Raffy, Physica (Amsterdam) **259–261B**, 567 (1999).
[7] H. Ding *et al.*, Phys. Rev. Lett. **76**, 1533 (1996).
[8] O. K. Andersen *et al.*, J. Phys. Chem. Solids **56**, 1573 (1995).
[9] S. Chakravarty *et al.*, Science **261**, 337 (1993).
[10] D. L. Feng *et al.*, Phys. Rev. Lett. **86**, 5550 (2001).
[11] Y. D. Chuang *et al.*, Phys. Rev. Lett. **87**, 117002 (2001).
[12] M. Randeria *et al.*, Phys. Rev. Lett. **74**, 4951 (1995).
[13] T. Valla *et al.* [Nature (London) **417**, 627 (2002)] have correlated ARPES data with c-axis transport in other layered oxides.
[14] J. C. Campuzano *et al.*, Phys. Rev. Lett. **83**, 3709 (1999).
[15] P. A. Lee and N. Nagaosa, Phys. Rev. B **46**, 5621 (1992).
[16] C. M. Varma, Phys. Rev. B **55**, 14 554 (1997).